Journal of Biomechanics 92 (2019) 137–145

Contents lists available at ScienceDirect

Journal of Biomechanics

journal homepage: www.elsevier.com/locate/jbiomech
www.JBiomech.com

A viscoelastic ellipsoidal model of the mechanics of plantar tissues

Jessica DeBerardinis [a,*], Janet S. Dufek [b], Mohamed B. Trabia [a]

[a] Department of Mechanical Engineering, University of Nevada, Las Vegas, United States
[b] Department of Kinesiology and Nutrition Sciences, University of Nevada, Las Vegas, United States

ARTICLE INFO

Article history:
Accepted 27 May 2019

Keywords:
Varying contact area models
Walking
Pressure-measuring insoles
Ground reaction force

ABSTRACT

Several assessments of the mechanics of plantar tissues, using various material models in conjunction with representing plantar regions using simple geometry, have been proposed. In this study, the plantar tissues were divided into eight regions to account for the various tissue characteristics. The plantar tissue model described each region as an ellipsoid, with a viscoelastic material model. The model combined varying elliptical contact areas with nonlinear tissue stiffness and damping. The main instruments used in this research were pressure-measuring insoles, which were used to determine the ground reaction force, as well as contact areas. The measured contact areas were fitted as elliptical areas to describe the compression of the corresponding ellipsoids. The approach was tested using walking data collected from 26 individuals: four men, 22 women, 24.4 ± 6.9 years old, 66.9 ± 21.4 kg of mass, 1.66 ± 0.12 m tall. The geometric and material variables of the proposed ellipsoidal model were optimized for each participant to match the ground reaction forces. Results suggest that the ellipsoid model is able to reproduce ground reaction force with reasonable accuracy. The largest errors were seen in heel and toe regions and were due to high-rate forces and small comparative areas, respectively. The model also showed that there are regional differences in the mechanical characteristics of plantar tissue, which confirms earlier research.

1. Introduction

Skin, fat, muscle, and tendons in the sole of the foot are collectively described as the plantar soft tissues. Each section of the foot has a unique functional structure (Sarrafian, 1993). For example, the rear foot (heel) tissues include a thick layer of subcutaneous connective tissue with fatty tissue pockets, which allow the rear foot to absorb the shock associated with the heel strike during walking or running. The midfoot plantar tissues are mainly composed of musculature and plantar fascia, which connect the calcaneus and metatarsal bones. These tissues help maintain postural balance, and work with other foot structures to generate movement. The forefoot plantar tissues are comprised mainly of muscles and tendons, with small fat pads underneath the metatarsal heads and toes. These tissues are used to push the foot off the ground in preparation for the subsequent step, during gait. While each of these plantar soft tissues exhibit different mechanical behaviors, researchers have most often proposed cumulative tissue models to describe the mechanical characteristics of plantar regions.

Several researchers (Gefen et al., 2001; Gilchrist and Winter, 1996; Scott and Winter, 1993), have used multiple, individual, nonlinear spring-damper systems across the plantar regions to model the plantar tissue's response to load. Spring-damper material models are computationally simple, which allow for quick calculations in comparison to more complex models. These models assume a point-load, which limits their applicability for studying the behavior of plantar tissues during walking. Another researcher (Neptune et al., 2000) used multiple, nonlinear spring-damper systems to represent the shoe sole and soft tissue and optimized techniques to improve the accuracy of the model.

Others have used hyperelastic material models to represent the nonlinearity of plantar tissues. Hyperelastic models examine the nonlinearity and elasticity of materials that have experienced large strains or deformations. They are beneficial to examine plantar tissue without the complexity of time-dependent, viscous effects. One such model is the Ogden model, which is a material model that develops a potential function of three constants, determined from experimental stress-strain data. This model was shown to be accurate in reproducing mechanical tests, but had errors in reproducing walking data (Budhabhatti et al., 2007; Chatzistergos et al., 2018; Chen et al., 2014; Chokhandre et al., 2012; Erdemir et al., 2006; Gu et al., 2010). Bucki et al. (2016), used a

* Corresponding author.
E-mail address: deberj1@unlv.nevada.edu (J. DeBerardinis).

https://doi.org/10.1016/j.jbiomech.2019.05.041
0021-9290/

Neo-Hookean model, which relates strain energy to the shear modulus, based on uniaxial stress strain data, in order to assess the plantar tissue of the full foot. The study found that the model's parameters needed to be participant-specific for greater accuracy. Hyperelastic polynomial strain functions have also been used to assess the plantar tissues during standing (Chen et al., 2010; Cheung et al., 2005). The accuracies of these hyperelastic material models were not evaluated under walking conditions. Further, the damping characteristics of the plantar tissues were not assessed.

Additionally, viscoelastic and hyper-viscoelastic material models of the plantar tissues have been developed (Behforootan et al., 2017; Cho et al., 2009; Fontanella et al., 2015, 2012; Forestiero et al., 2015; Qian et al., 2013). These models consider the viscous and elastic characteristics of plantar tissues such as incompressibility, nonlinear stress-strain, and time-dependent effects. This allows for a more accurate model of the plantar tissue. The results of these models also showed the need for participant specific models and the ability to measure the kinetics on the foot tissue. Moreover, the models were specific to particular plantar locations and the finite element models required static scans of the foot to develop the model.

Material models of plantar tissues that include varying contact areas can aid in assessing the behavior of these tissues during walking. These models allow for an additional level of complexity in comparison to the point-load models. But, the computational simplicity is maintained as researchers have used several geometric shapes for varying contact area models. Güler et al. (1998) used a viscoelastic sphere to model the heel. This model was able to reproduce low-load heel compression experiments at various loading velocities. Pàmies-Vilà et al. (2014) used several viscoelastic spheres, one placed in the rearfoot and three distributed across the rest of the foot, which were optimized to the data of a single participant's walking. Similarly, Shourijeh and McPhee (2015) used several spheres to model the heel, metatarsals, and toes. Each sphere was associated with different nonlinear stiffness and damping values. The parameters of the model were optimized based on data collected from the right foot of a single participant's walking. Millard and Kecskeméthy (2015) modeled the heel and forefoot plantar tissues using circular disks, coupled with a Hunt-Crossly contact model and nonlinear stiffness. This model was accurate in representing the kinematic results, but generated larger errors in reproducing the kinetic data. Lopes et al., (2015), used six, nonlinear, super-ellipsoid contact elements to determine three-dimensional foot-ground contact forces within a shoe. The super-ellipsoid model results were compared to multiple, point-contact, viscoelastic models. It was found that the super-ellipsoid model was found to be equally as accurate as the point-contact models and more computationally efficient. Brown and McPhee, (2018) used volumetric ellipsoid contact models, defined by linear springs and dampers, to assess the heel, metatarsals, and hallux. The parameters of the models (geometry of the three ellipsoids and global stiffness and damping) were optimized based on the motion capture analysis and center of pressure coordinates. The parameters were used to reproduce the plantar pressure and ground reaction force but were inaccurate.

In this study, a new model was developed and tested to assess the mechanics of plantar tissues during walking. This model is characterized as a viscoelastic material model, with nonlinear stiffness and nonlinear damping. Plantar tissues were divided into eight regions, each represented by an ellipsoid, in order to account for the change in material behavior between and among regions. This will create a hybrid between a viscoelastic and varying contact area model. The accuracy of the developed model in duplicating the normal components of ground reaction force and contact area during walking was tested.

2. Methods

2.1. Viscoelastic ellipsoidal model of the plantar tissues

2.1.1. Kinematics

The plantar tissues were represented by a sequence of ellipsoids placed at key plantar regions. In this study, the plantar region was divided as follows: Heel, Posterior Midfoot, Anterior Midfoot, Metatarsals 1–2, Metatarsals 3–5, Hallux, Toe 2, and Toes 3–5. The ellipsoids were fitted to the areas of the foot that were in contact with the ground (Fig. 1) While a less detailed division is possible, the authors chose to pursue this division in order to identify regions with significant changes in stiffness or damping.

Fig. 2 shows the ellipsoidal model that was developed. The major radii of the ellipsoid were A, B, and C in the X, Y, and Z directions, respectively. At any time instant, the tissue deformation, d, was associated with an elliptical contact area, A_e. This area had two major radii, r_A and r_B (Fig. 3).

The elliptical radii were expressed as:

$$r_A = \frac{A\sqrt{2Cd - d^2}}{C} \tag{1}$$

$$r_B = \frac{B\sqrt{2Cd - d^2}}{C} \tag{2}$$

Any point on the contact area plane was defined using the ellipsoid equation, which was then solved to determine the tissue deformation of this point, δ :

$$\delta = d - C + \sqrt{C^2 - \rho^2(2Cd - d^2)} \tag{3}$$

The above equation was differentiated to obtain the rate of change of tissue deformation, $\dot{\delta}$:

$$\dot{\delta} = \dot{d}\left(1 - \frac{\rho^2(C - d)}{\sqrt{C^2 - 2C\rho^2 d + \rho^2 d^2}}\right) \tag{4}$$

2.1.2. Kinetics

Following Güler et al. (1998), this research used a viscoelastic material with nonlinear stiffness and damping, k and c, respectively. These variables were defined as:

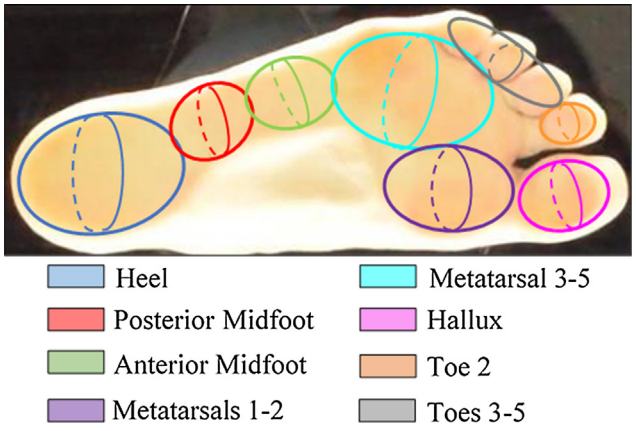

Fig. 1. An example of the placement of the ellipsoid models representing the foot. The ellipsoids were placed where the foot contacts the ground, separated into the following regions: Heel (blue), Posterior Midfoot (red), Anterior Midfoot (green), Metatarsals 1–2 (purple), Metatarsals 3–5 (teal), Hallux (pink), Toe 2 (orange), Toes 3–5 (gray). (For interpretation of the references to colour in this figure legend, the reader is referred to the web version of this article.)

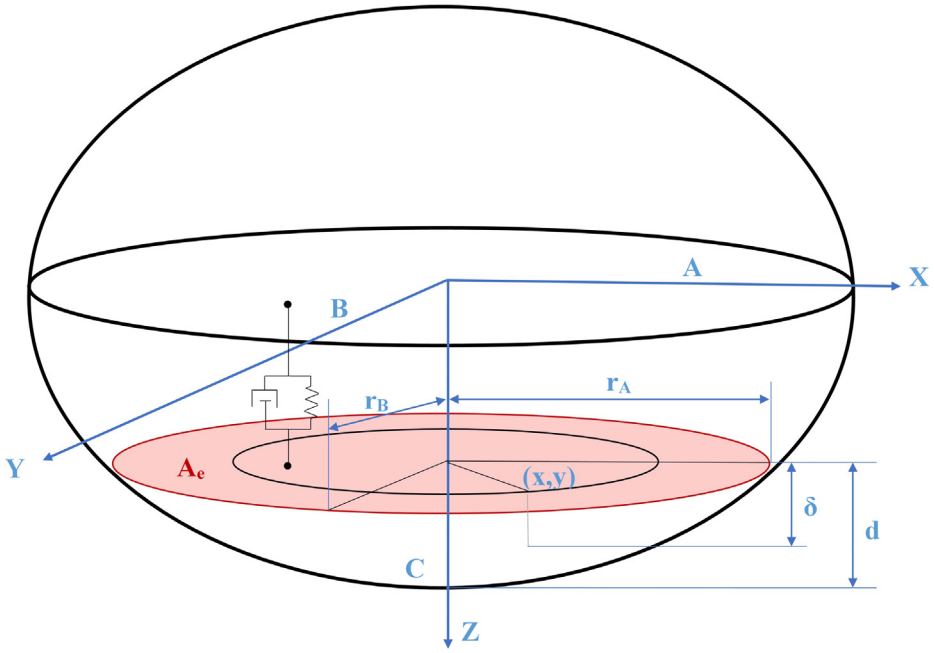

Fig. 2. A dimensional representation of the ellipsoidal model. *A*, *B*, and *C* represent the major radii of the ellipsoid, which are centered at the origins of *X*, *Y*, and *Z*. The total deformation is represented by *d*, with δ representing the local deformation at coordinate (*x*, *y*).

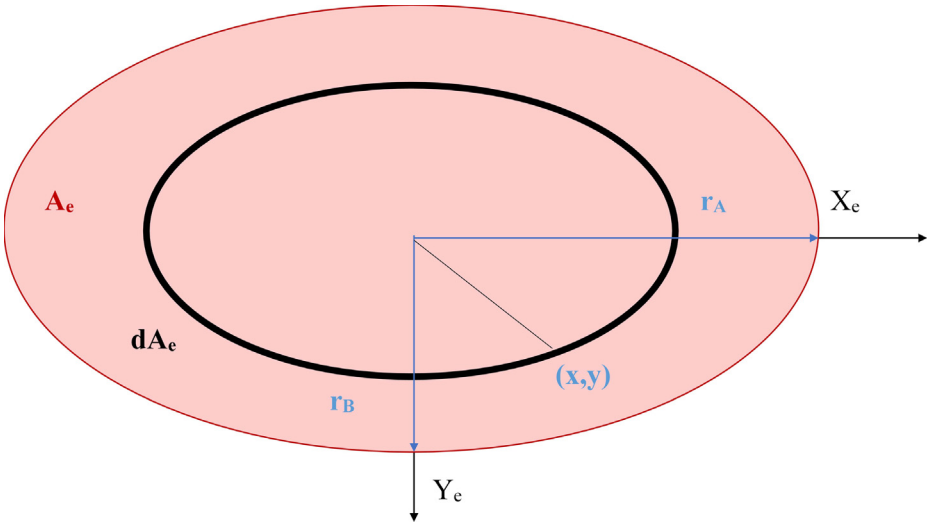

Fig. 3. The elliptical contact area A_e with radii r_A and r_B. The point (*x*, *y*) is the location of the local deformation and dA_e is the differential element of the contact area.

$$k = \overline{k}\left(\frac{d}{d_0}\right)^n \tag{5}$$

$$c = \overline{c}\left(\frac{d}{d_0}\right)^m \tag{6}$$

where d denotes tissue deformation, d_0 the original thickness of the plantar tissue, $\overline{k}$ the stiffness coefficient, n the positive stiffness exponent, $\overline{c}$ the damping stiffness coefficient, and m the positive damping exponent. When a vertical ground reaction force component, F_z, was applied to a plantar tissue ellipsoid, it induced an internal reaction that can be described as:

$$F_z = \int_{A_e}\left(k\delta + c\dot{\delta}\right)dA_e \tag{7}$$

It may be suitable to express the above integral in terms of the distorted polar coordinates (Strickland, 2012):

$$x = \rho(r_A\cos(\theta)) \tag{8}$$

$$y = \rho(r_B\sin(\theta)) \tag{9}$$

where θ denotes the angle of rotation around the z axis in the contact plane ($0 \le \theta \le 2\pi$), and ρ the ratio of the radii of the elliptical contact area ($0 \le \rho \le 1$).

Based on this approach, the differential of the area, dA_e, was expressed as (Hass et al., 2016):

$$dA_e = \left|\frac{\partial(x,y)}{\partial(\rho,\theta)}\right| d\theta d\rho \tag{10}$$

The force balance became:

$$F_z = \int_0^1\int_0^{2\pi}\left(k\delta + c\dot{\delta}\right)(\rho r_A r_b d\theta d\rho) \tag{11}$$

or,

$$F_z = \int_0^1 \int_0^{2\pi} \left(k\delta + c\dot{\delta}\right)\left(\rho \frac{ABd(2C-d)}{C^2} d\theta d\rho\right) \tag{12}$$

substituting the kinematic equations and simplifying,

$$F_z = \frac{ABd\pi}{C}\left(\bar{k}\left(\frac{d}{d_0}\right)^n d\left(1-\frac{d}{3C}\right) + \bar{c}\left(\frac{d}{d_0}\right)^m \dot{d}\left(\frac{6C^2-4Cd+d^2}{3C(2C-d)}\right)\right) \tag{13}$$

2.1.3. Modification to fit pressure-measuring insoles

The model was expressed in terms of the deformation, d, of the ellipsoid. However, directly measuring the deformation during walking is challenging. Instead, the authors used the contact area associated with the deformation, as it can be measured using pressure-measuring insoles. Therefore, the deformation d was expressed in terms of the contact area based on the equation of the ellipsoid, A_e as:

$$d = C\left(1-\sqrt{1-\frac{A_e}{\pi AB}}\right) \tag{14}$$

The deformation rate, $\dot{d}$, was expressed as:

$$\dot{d} = \frac{C}{\pi AB}\left(\frac{\dot{A}_e}{\sqrt{1-\frac{A_e}{\pi AB}}}\right) \tag{15}$$

Using the finite difference rule, $\dot{d}$ could be expressed as:

$$\dot{d}_i \approx \frac{C\left(\sqrt{1-\frac{A_{e_i}}{\pi AB}} - \sqrt{1-\frac{A_{e_{i+1}}}{\pi AB}}\right)}{t_{i+1}-t_i} \tag{16}$$

where i denotes the current time instance, t_i.

2.2. Pressure-measuring insoles

Medilogic® pressure-measuring insoles in European sizes 35–45 (Medilogic T&T, Schönefeld, Germany) were used as the main instruments in this research. These insoles were used to simultaneously measure the ground reaction force and plantar contact area during walking (DeBerardinis et al., 2018a; Lidstone et al., 2019). The insole sensors were grouped into eight regions, which correspond to those shown in Fig. 1. An example of the sensor division is shown in Fig. 4. This division of the midfoot allowed for a more accurate representation of the arch, since a single ellipse fitted over the entire midfoot would lead to larger error.

Medilogic® pressure-measuring insoles were used to measure force and area, which had been validated previously; the contact area of the insole sensors was then used to determine the elliptical contact area, which had also been shown as accurate (DeBerardinis et al., 2018b; Lopes et al., 2015). The elliptical contact area drove the placement of the ellipsoids across the plantar surface. As the ellipses were fitted using a Matlab code that would provide the center and rotation of the elliptical contact area (Brown, 2007). The center of the corresponding ellipsoid was directly above the center of the contact ellipse and with the same rotation. The ellipsoid radii that determined the size and distance from the floor were optimized, which is discussed in Section 2.5.

2.3. Insole data preprocessing

The plantar contact area and ground reaction force data were expressed mathematically for use in the proposed model. Because of the relatively limited number of sensors, the area curves were not typically smooth. Therefore, the data were smoothed using a three-point moving average, followed by a 5th order polynomial curve fitting (Fig. 5a). In contrast, the force-time curve had a better resolution, since it was the result of the contributions of many sensors. Therefore, the data were fitted with a 5th order polynomial directly (Fig. 5b).

2.4. Data collection

Ground reaction force and plantar contact area data were collected from 26 healthy participants (four men, 22 women, 24.4 ± 6.9 years old, 66.9 ± 21.4 kg of mass, 1.66 ± 0.12 m tall), who consented to participate (IRB #724468). Each participant was asked to wear a pair of insoles, fitted to their foot sizes, inside a pair of socks. The demographics, with respect to insole size, are shown in Table 1. The participants were asked to sit and lift both

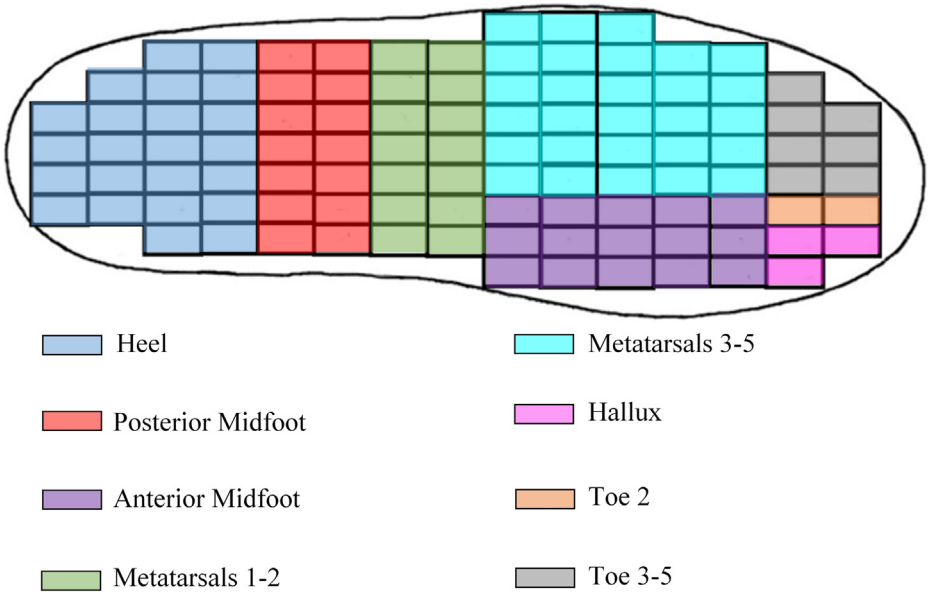

Fig. 4. The division of the insole sensors into eight regions: Heel (blue), Posterior Midfoot (red), Anterior Midfoot (green), Metatarsals 1–2 (purple), Metatarsals 3–5 (teal), Hallux (pink), Toe 2 (orange), Toes 3–5 (gray). (For interpretation of the references to colour in this figure legend, the reader is referred to the web version of this article.)

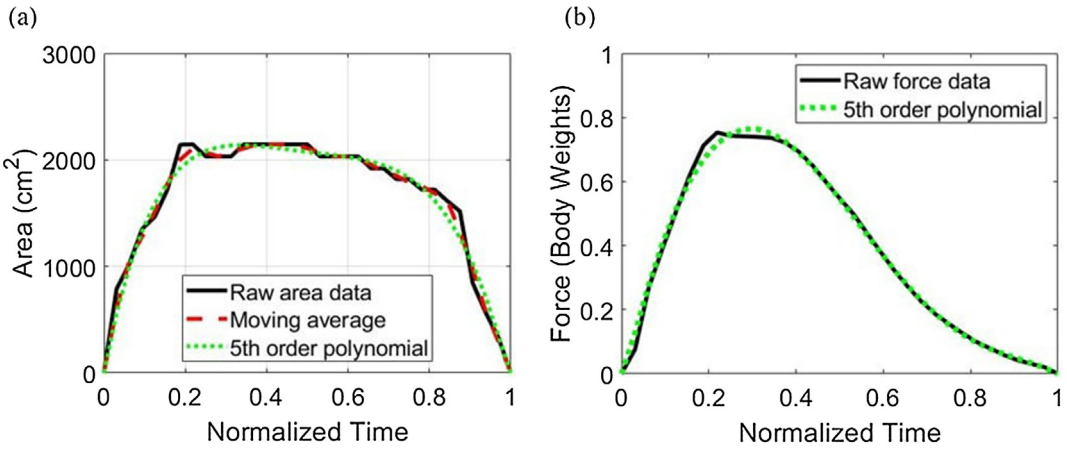

Fig. 5. A set of exemplar area-time and force-time curves for the heel: (a) the area raw data is smoothed with a moving average, and then fit with a 5th order polynomial; (b) the force raw data fit with a 5th order polynomial.

Table 1
The demographic data of the participants, separated by insole size, shown as average (standard deviation).

Insole size (Eur)	Female/Male	Age (yrs)	Mass (kg)	Height (m)
35–36	5/0	21.6 (0.9)	48.9 (6.0)	1.56 (0.07)
37–38	8/0	22.3 (2.5)	55.1 (5.6)	1.58 (0.06)
39–40	5/0	24.4 (2.6)	75.3 (18.6)	1.64 (0.03)
41–42	3/0	21.6 (1.7)	84.8 (7.2)	1.81 (0.09)
43–44	2/1	33.9 (15.4)	82.8 (34.8)	1.76 (0.05)
45–46	0/2	29.9 (1.5)	86.8 (14.3)	1.84 (0.01)

feet off the floor for five seconds, stand and remain stationary for 10 s, and then sit again and lift both feet off the floor for five seconds in order to identify the output of the insoles under non-weight bearing conditions. Participants were then asked to walk in a straight path for five meters at a self-selected speed. One step, for each foot, was isolated, and sensor data were processed as described earlier. The experiment was repeated for three trials.

2.5. Identification of the plantar tissues viscoelastic ellipsoidal model of each participant

It was expected that the plantar tissues of the participants would vary. Therefore, the tissue model parameter values of each plantar region had to be identified for each participant separately. For each region, the variables to be identified were:

$$x \in \left(A, B, C, d_0, \overline{k}, n, \overline{c}, m\right) \tag{17}$$

The values of these variables were identified for each region by tuning them, so that the calculated model force matched the ground reaction force portion that was carried by each region. This was achieved by minimizing the sum of the squared difference between the measured ground reaction force and the output model signal at each footpad region (Eq. (18)) using the Matlab *fmincon* function (MathWorks, 2018).

$$Minimize: \quad O_{i,j,k}(x) = \sum_{t=1}^{n} \left(FE_{i,j,k}(t) - FM_{i,j,k}(x,t)\right)^2 \tag{18}$$

where $O_{i,j,k}$ denotes the objective function of plantar region j of limb k for participant i; $FE_{i,j,k}(t)$ denotes the measured ground reaction force of plantar region j of limb k for participant i at time instant t; $FM_{i,j,k}(x,t)$ denotes the ground reaction force output of the model of plantar region j of limb k for participant i at time instant t; and n denotes the number of total time instants when plantar region j of limb k for participant i was active.

A penalty term, P, was added to the force output of the model to ensure that the choice of parameters within the search would not yield a negative value of vertical ground reaction force (Eq. (19)), which cannot physically occur:

$$FM_{i,j,k}(x,t) = \begin{cases} FM_{i,j,k}(x,t) & if \;\; FM_{i,j,k}(x,t) \geq 0 \\ FM_{i,j,k}(x,t) + P\left(FM_{i,j,k}(x,t)\right)^2 & if \;\; FM_{i,j,k}(x,t) < 0 \end{cases} \tag{19}$$

Lower and upper bounds constraints were applied to the geometric and material variables. These constraints were specific to each insole size, were based on previous measurements of plantar tissue thickness (Thomas et al., 2004; Uzel et al., 2006; Valiant, 1984; Zheng et al., 2000), and variables of the plantar tissue material models (Güler et al., 1998; Shourijeh and McPhee, 2015). These constraints were included in the variable search using the *interior-point* algorithm. If a variable violated the bounds, the search directed it back to the feasible space, using an interior penalty function (MathWorks, 2018). Appendix A contains the lower and upper bounds of the variables used in this research.

3. Results

Fig. 6 displays the typical ground reaction force experimental results, along with the typical model outputs, divided between plantar regions. As the figure shows, the proposed model was able to match the experimental data substantially. The greatest deviations were seen in the heel and toes. It is also possible that the overlap of the ellipsoid elements led to systematic errors which could lead to larger errors when more ellipsoids are contributing to the contact force estimation.

To assess the effectiveness of the proposed plantar tissue model in capturing the experimental force signal, the root mean square

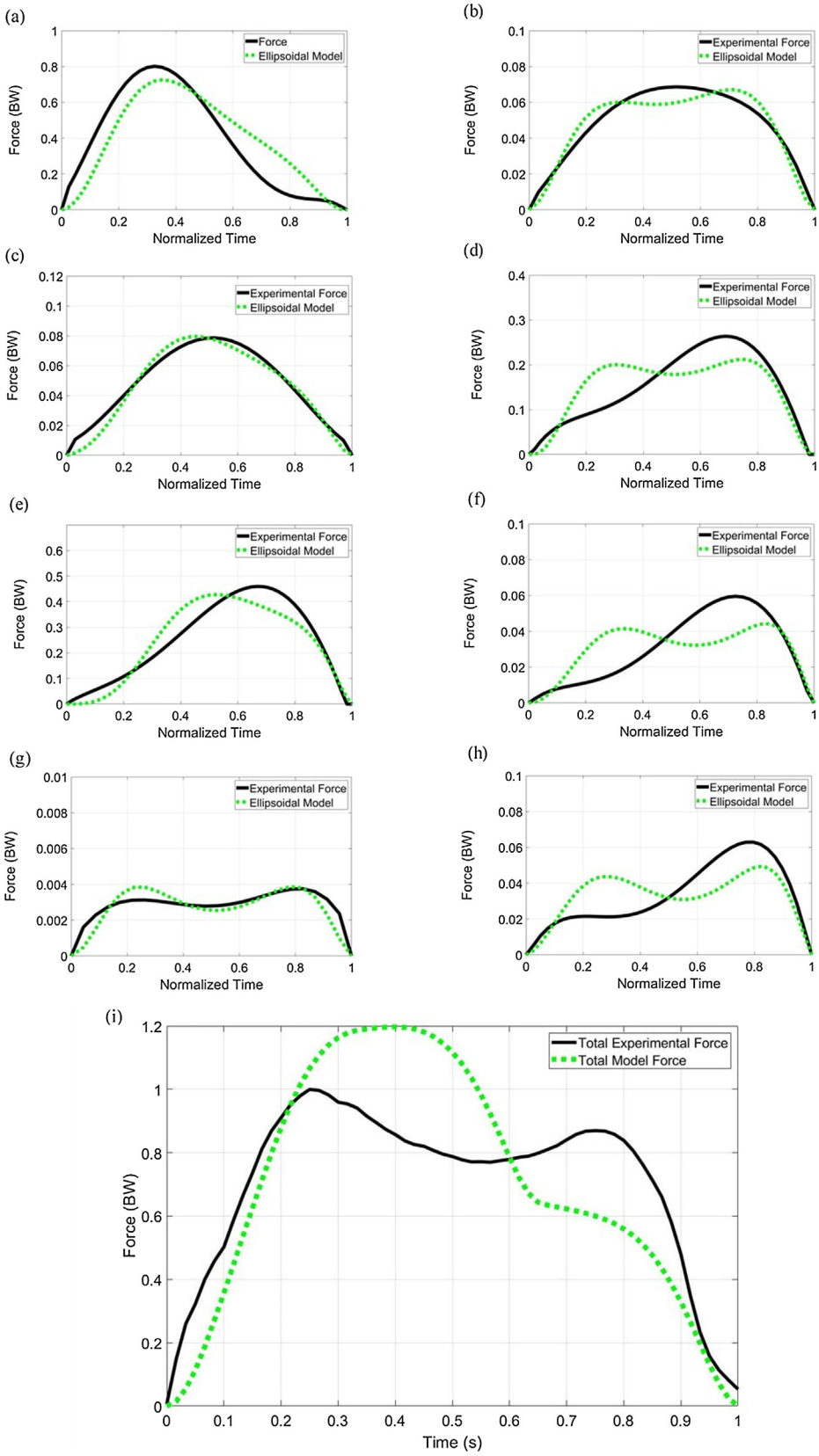

Fig. 6. Typical results of the model for each region compared to the experimental ground reaction force for the right foot of a participant wearing insole size 37–38. The graphs correspond to the following plantar regions: (a) Heel, (b) Midfoot Posterior, (c) Midfoot Anterior, (d) Metatarsals 1–2, (e) Metatarsals 3–5, (f) Hallux, (g) Toe 2, (h) Toes 3–5, and (i) the combined experimental and model forces.

Table 2
The NRSME results of exemplar data from the right foot of a participant wearing a size 37–38 insole.

Plantar region	NRSME
Heel	22.1%
Midfoot Posterior	6.1%
Midfoot Anterior	8.2%
Metatarsals 1–2	18.1%
Metatarsals 3–5	11.7%
Toe 1	24.5%
Toe 2	13.9%
Toes 3–5	20.9%

error, normalized with respect to the maximum experimental force of each plantar region, was calculated:

$$NRMSE_{i,j,k} = \frac{\sqrt{\frac{O_{i,j,k}(x)}{n}}}{\max\left(FE_{i,j,k}\right)} \tag{20}$$

The normalized root mean square error (NRMSE) results for the three trials and two limbs of each participant (six data sets total), were averaged for each participant. These results were then averaged again for each plantar region of each insole size. Standard deviations were calculated to determine the consistency of the

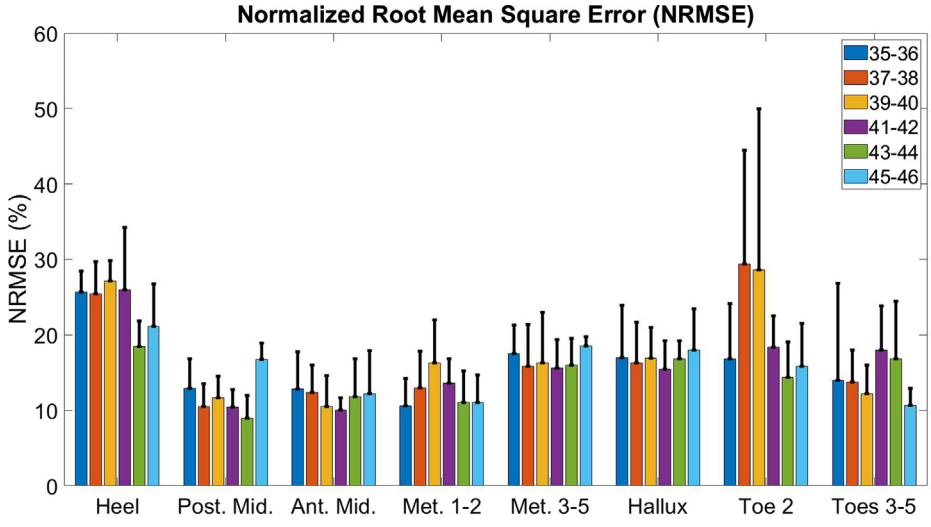

Fig. 7. The NRSME results for each plantar region and insole size.

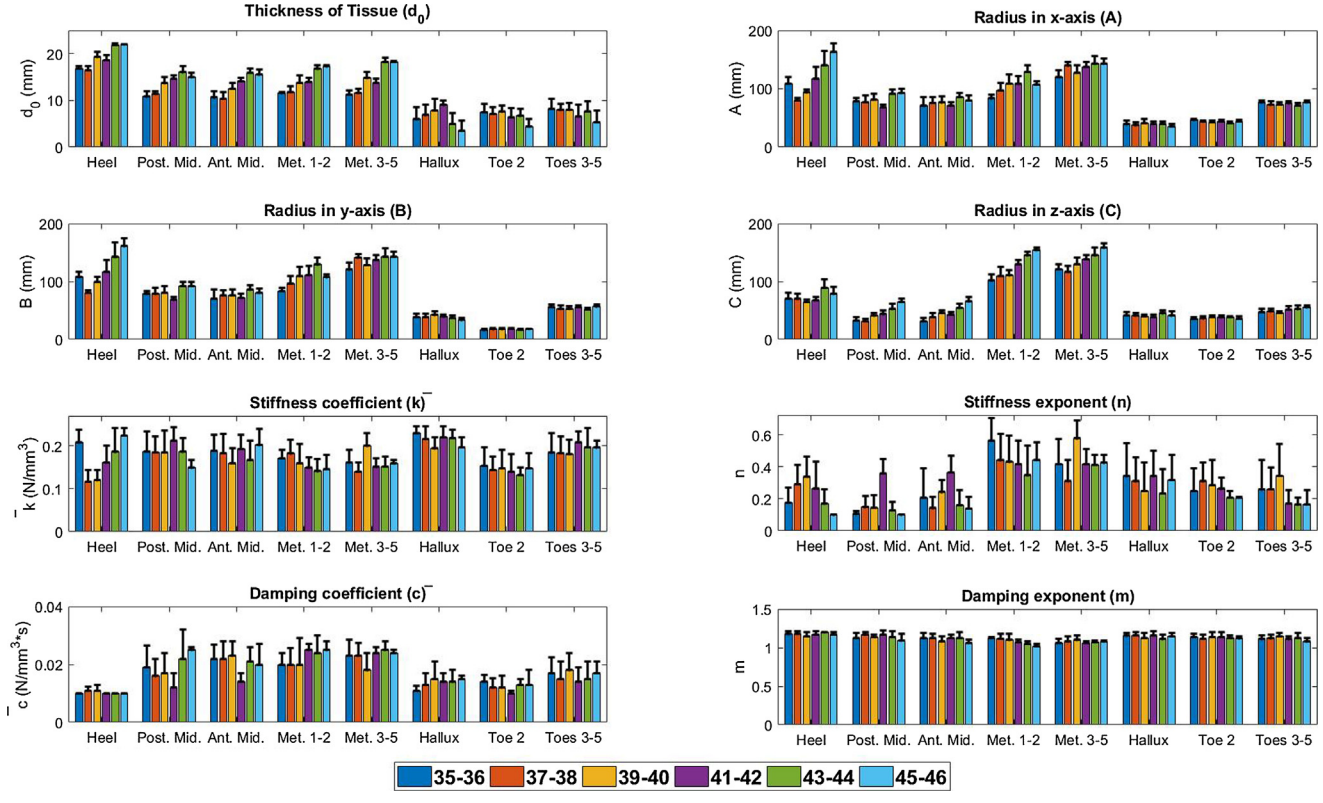

Fig. 8. The average and standard deviation for the plantar tissue model variables: (a) tissue thickness, (b) radius in x-axis, (c) radius in y-axis, (d) radius in z-axis, (e) stiffness, (f) stiffness coefficient, (g) damping, and (h) damping coefficient. Values are displayed for each insole size and plantar region.

results for each insole size and to assess the feasibility of the proposed tissue model. The NRMSE results of Fig. 6 are shown in Table 2. The NRMSE results for all participants and insole sizes are shown in Fig. 7.

Further, the results of the applied viscoelastic ellipsoid plantar tissue model were combined for the three trials and two limbs of each participant (six data sets per participant) to calculate an average set of variables $\left(A, B, C, d_0, \overline{k}, n, \overline{c}, m\right)$ for each plantar region for that participant. These results were then averaged again for each insole size, Fig. 8.

4. Discussion

The results of Figs. 6 and 7 and Table 2 indicated that the ellipsoid model was able to reproduce the vertical ground reaction force in each region, with varying degrees of accuracy. It was observed that there was a relatively small variation in the errors, despite having several different participants for each insole size, which indicates that the model was robust. The errors were the largest in the heel and the toe regions, particularly Toe 2. Additionally, all toe regions had larger standard deviations than the other plantar regions. The heel region may have had larger errors due to the comparatively high forces seen at heel strike, which might not allow for accurate modeling. On the other hand, the errors and standard deviations associated with the measurements of the toe regions might have been due to the limited number of sensors available (smaller comparative area) to record the kinetic data.

As Fig. 8 shows, the geometric variables (d_0, A, B, and C) increased with insole size. It was also found that the radii of the ellipsoid were the largest for the metatarsals followed by the heel, which are the largest plantar regions of the foot. The results further indicated that the plantar regions had a circular cross-section (A and B were close), while the radii in the z-axis (C) was significantly smaller, which demonstrated that the spherical models proposed earlier had a limited ability to describe the various plantar regions (Güler et al., 1998; Pàmies-Vilà et al., 2014; Shourijeh and McPhee, 2015). The model predicted that plantar tissues were the thickest at the heel, followed by the metatarsals and midfoot for all insole sizes. These results were consistent with the values measured previously (Thomas et al., 2004; Uzel et al., 2006; Valiant, 1984; Zheng et al., 2000).

The material model variables $\left(\overline{k}, n, \overline{c}, m\right)$ of Fig. 8, indicated that each plantar region had different stiffness and damping characteristics, demonstrating that general foot models, or models that combine multiple plantar regions, might lead to inaccuracies. These results showed that while $\overline{k}$ was fairly uniform for all plantar regions and insole sizes, n was the highest at the metatarsal regions, indicating that these regions had the highest tissue stiffness. These results were comparable to those found using load-unload or ultrasound elastography (Thomas et al., 2004; Zheng et al., 2000). On the other hand, while m was uniform for all plantar regions and insole sizes, $\overline{c}$ was the highest at the midfoot and metatarsal regions, indicating that these regions had the highest energy absorption. These values were smaller than those reported by Güler et al., (1998), demonstrating the importance of using gait data, rather than limiting data to what can be collected when participants are standing, or have their feet in the air.

A limitation of this model is that it was necessary to assume that the plantar tissue was homogeneous and did not distinguish the various tissues involved during walking. It is possible that the differences in the material model variables could be due to differences in anatomical structure in addition to differences in tissue material properties. However, these differences can still be used to track changes in the tissue structure and material characteristics in pathological tissue.

5. Conclusion

A model describing the mechanical behavior of plantar tissues during walking was developed and tested. Plantar tissues were divided into eight regions, each represented by an ellipsoid to account for varying plantar geometry. It was assumed that plantar tissue material is viscoelastic, with both nonlinear stiffness and damping. Variation of the contact area during walking was included in the model. The accuracy of the proposed plantar tissue model was assessed by comparing its output to the measurement of the ground reaction force during walking. This was measured for participants wearing six different sizes of pressure-measuring insoles, with each best matched to the foot size of the participant.

The proposed model was fairly successful in producing ground reaction force during walking, as well as characterizing footpad thickness, stiffness, and damping. However, results could be further enhanced in the future by using insoles with a larger number of sensors, and by using including the nonlinearity of the sensors. Future work may incorporate new shapes, such as super-ellipsoids, or different ellipsoid layouts to be more specific to the various regions of the foot. Additionally, the proposed model along with clinical data collected from persons with plantar diseases such as diabetes, plantar fasciitis, chronic pain, etc., in order to predict and/or prevent such plantar diseases.

Contributions

Author JDB collected the data, developed the model, assessed the results, and wrote the manuscript. JSD and MBT both advised JDB on the experiment and model development. JSD and MBT also edited and revised the manuscript.

Declaration of Competing Interest

There are no conflicts of interest.

Acknowledgements

The authors would like to acknowledge funding from the Barrick Graduate Research Fellowship, from the University of Nevada, Las Vegas, United States for the funding of this research.

Appendix A. Supplementary material

Supplementary data to this article can be found online at https://doi.org/10.1016/j.jbiomech.2019.05.041.

References

Behforootan, S., Chatzistergos, P.E., Chockalingam, N., Naemi, R., 2017. A clinically applicable non-invasive method to quantitatively assess the visco-hyperelastic properties of human heel pad, implications for assessing the risk of mechanical trauma. J. Mech. Behav. Biomed. Mater. 68, 287–295. https://doi.org/10.1016/j.jmbbm.2017.02.011.

Brown, P., McPhee, J., 2018. A 3D ellipsoidal volumetric foot–ground contact model for forward dynamics. Multibody Syst. Dyn. 42, 447–467. https://doi.org/10.1007/s11044-017-9605-4.

Brown, R., 2007. FITELLIPSE: Least squares ellipse fitting.

Bucki, M., Luboz, V., Perrier, A., Champion, E., Diot, B., Vuillerme, N., Payan, Y., 2016. Clinical workflow for personalized foot pressure ulcer prevention. Med. Eng. Phys. 38, 845–853. https://doi.org/10.1016/j.medengphy.2016.04.017.

Budhabhatti, S.P., Erdemir, A., Petre, M., Sferra, J., Donley, B., Cavanagh, P.R., 2007. Finite element modeling of the first ray of the foot: A tool for the design of interventions. J. Biomech. Eng. 129, 750. https://doi.org/10.1115/1.2768108.

Chatzistergos, P.E., Behforootan, S., Allan, D., Naemi, R., Chockalingam, N., 2018. Shear wave elastography can assess the in-vivo nonlinear mechanical behavior of heel-pad. J. Biomech. 1–7. https://doi.org/10.1016/J.JBIOMECH.2018.09.003.

Chen, W.-M., Lee, S.-J., Lee, P.V.S., 2014. The in vivo plantar soft tissue mechanical property under the metatarsal head: implications of tissues' joint-angle

dependent response in foot finite element modeling. J. Mech. Behav. Biomed. Mater. 40, 264–274. https://doi.org/10.1016/j.jmbbm.2014.09.007.
Chen, W.-M., Lee, T., Lee, P.V.-S., Lee, J.W., Lee, S.-J., 2010. Effects of internal stress concentrations in plantar soft-tissue—A preliminary three-dimensional finite element analysis. Med. Eng. Phys. 32, 324–331. https://doi.org/10.1016/j.medengphy.2010.01.001.
Cheung, J.T.M., Zhang, M., Leung, A.K.L., Fan, Y.B., 2005. Three-dimensional finite element analysis of the foot during standing - A material sensitivity study. J. Biomech. 38, 1045–1054. https://doi.org/10.1016/j.jbiomech.2004.05.035.
Cho, J.R., Park, S.B., Ryu, S.H., Kim, S.H., Lee, S.B., 2009. Landing impact analysis of sports shoes using 3-D coupled foot-shoe finite element model. J. Mech. Sci. Technol. 23, 2583–2591. https://doi.org/10.1007/s12206-009-0801-x.
Chokhandre, S., Halloran, J.P., van den Bogert, A.J., Erdemir, A., 2012. A three-dimensional inverse finite element analysis of the heel pad. J. Biomech. Eng. 134, 031002. https://doi.org/10.1115/1.4005692.
DeBerardinis, J., Dufek, J.S., Trabia, M.B., Lidstone, D.E., 2018a. Assessing the validity of pressure-measuring insoles in quantifying gait variables. J. Rehabil. Assist. Technol. Eng. Special Co, 1–12.
DeBerardinis, J., Lidstone, D., Dufek, J.S., Trabia, M.B., 2018b. Elliptical estimation of plantar contact areas during walking. Annual Meeting of the American Society of Biomechanics. Minneapolis.
Erdemir, A., Viveiros, M.L., Ulbrecht, J.S., Cavanagh, P.R., 2006. An inverse finite-element model of heel-pad indentation. J. Biomech. 39, 1279–1286. https://doi.org/10.1016/j.jbiomech.2005.03.007.
Fontanella, C.G., Forestiero, A., Carniel, E.L., Natali, A.N., 2015. Investigation of the mechanical behaviour of the plantar soft tissue during gait cycle: Experimental and numerical activities. Proc. Inst Mech. Eng. Part H J. Eng. Med. 229, 713–720. https://doi.org/10.1177/0954411915601702.
Fontanella, C.G., Matteoli, S., Carniel, E.L., Wilhjelm, J.E., Virga, a., Corvi, a., Natali, a. N., 2012. Investigation on the load-displacement curves of a human healthy heel pad: In vivo compression data compared to numerical results. Med. Eng. Phys. 34, 1253–1259. https://doi.org/10.1016/j.medengphy.2011.12.013.
Forestiero, A., Raumer, A., Carniel, E.L., Natali, A.N., 2015. Investigation of the interaction phenomena between foot and insole by means of a numerical approach. Proc. Inst. Mech. Eng. Part P J. Sport. Eng. Technol. 229, 3–9. https://doi.org/10.1177/1754337114560579.
Gefen, A., Megido-Ravid, M., Itzchak, Y., 2001. In vivo biomechanical behavior of the human heel pad during the stance phase of gait. J. Biomech. 34, 1661–1665.
Gilchrist, L.A., Winter, D.A., 1996. A two-part, viscoelastic foot model for use in gait simulations. J. Biomech. 29, 795–798. https://doi.org/10.1016/0021-9290(95)00141-7.
Gu, Y., Li, J., Ren, X., Lake, M.J., Zeng, Y., 2010. Heel skin stiffness effect on the hind foot biomechanics during heel strike. Skin Res. Technol. 16, 291–296. https://doi.org/10.1111/j.1600-0846.2010.00425.x.
Güler, H.C., Berme, N., Simon, S.R., 1998. A viscoelastic sphere model for the representation of plantar soft tissue during simulations. J. Biomech. 31, 847–853. https://doi.org/10.1016/S0021-9290(98)00085-2.
Hass, J., Weir, M.D., Thomas, G.B.J., Heil, C., 2016. Substitutions in multiple integrals. In: Hoag, C., Lynch, D., Hoffman, W., Casha, S., Al., E. (Eds.), University Calculus: Early Transcendentals. Pearson, London, pp. 806–808.
Lidstone, D.E., DeBerardinis, J., Dufek, J.S., Trabia, M.B., 2019. Electronic measurement of plantar contact area during walking using an Adaptive Thresholding Method for Medilogic® Pressure-measuring insoles. Foot 39, 1–10. https://doi.org/10.1016/j.foot.2019.01.009.
Lopes, D.S., Neptune, R.R., Ambrósio, J.A., Silva, M.T., 2015. A superellipsoid-plane model for simulating foot-ground contact during human gait. Comput. Methods Biomech. Biomed. Engin. 19, 954–963. https://doi.org/10.1080/10255842.2015.1081181.
MathWorks, 2018. fmincon [WWW Document]. Documentation. URL https://www.mathworks.com/help/optim/ug/fmincon.html.
Millard, M., Kecskeméthy, A., 2015. A 3D foot-ground model using disk contacts. Mech. Mach. Sci. 26, 161–169. https://doi.org/10.1007/978-3-319-10723-3_17.
Neptune, R.R., Wright, I.C., van den Bogert, A.J., 2000. A method for numerical simulation of single limb ground contact events: Application to heel-toe running. Comput. Methods Biomech. Biomed. Engin. 3, 321–334. https://doi.org/10.1080/10255840008915275.
Pàmies-Vilà, R., Font-Llagunes, J.M., Lugrís, U., Cuadrado, J., 2014. Parameter identification method for a three-dimensional foot-ground contact model. Mech. Mach. Theory 75, 107–116. https://doi.org/10.1016/j.mechmachtheory.2014.01.010.
Qian, Z., Ren, Lei, Ding, Y., Hutchinson, J.R., Ren, Luquan, 2013. A dynamic finite element analysis of human foot complex in the sagittal plane during level walking. PLoS One 8, 1–10. https://doi.org/10.1371/journal.pone.0079424.
Sarrafian, S.K., 1993. Anatomy of the Foot and Ankle: Descriptive, Topographic, Functional. J.B. Lippincott Company, Philadelphia.
Scott, S.H., Winter, D.A., 1993. Biomechanical model of the human foot: Kinematics and kinetics during the stance phase of walking. J. Biomech. 26, 1091–1104. https://doi.org/10.1016/S0021-9290(05)80008-9.
Shourijeh, M.S., McPhee, J., 2015. Foot–ground contact modeling within human gait simulations: from Kelvin-Voigt to hyper-volumetric models. Multibody Syst. Dyn. 35, 393–407. https://doi.org/10.1007/s11044-015-9467-6.
Strickland, N., 2012. Compute double integrals in polar coordinates [WWW Document]. URL http://neil-strickland.staff.shef.ac.uk/courses/MAS243/lectures/handout07.pdf.
Thomas, V.J., Patil, K.M., Radhakrishnan, S., 2004. Three-dimensional stress analysis for the mechanics of plantar ulcers in diabetic neuropathy. Med. Biol. Eng. Comput. 42, 230–235. https://doi.org/10.1007/BF02344636.
Uzel, M., Cetinus, E., Ekerbicer, H.C., Karaoguz, A., 2006. Heel pad thickness and athletic activity in healthy young adults: A sonographic study. J. Clin. Ultrasound 34, 231–236. https://doi.org/10.1002/jcu.
Valiant, G.A., 1984. A Determination of the Mechanical Characteristics of the Human Heel Pad In Vivo. The Pennsylvania State University.
Zheng, Y., Choi, Y.K., Wong, K., Chan, S., Mak, A.F., 2000. Biomechanical Assessment of Plantar Foot Tissue in Diabetic Patients using an Ultrasound Indentation System. Ultrasound Med. Biol. 26, 1–20.